ACKNOWLEDGMENT

The author wishes to thank Prof. J. Herve, Université de Provence (Centre de Saint-Jérôme) and G. Convert, Laboratoire Central Thomson-C.S.F., for many helpful discussions. He also wishes to thank Mr. Mailhan for his technical assistance.

REFERENCES

[1] M. Dean and M. J. Howes, "*J* band transferred-electron oscillators," *IEEE Trans. Microwave Theory Tech.*, vol. MTT-21, pp. 121–127, Mar. 1973.
[2] D. Cawsey, "Wide-range tuning of solid-state microwave oscillators," *IEEE J. Solid-State Circuits* (Corresp.), vol. SC-5, pp. 82–84, Apr. 1970.
[3] *Gunn Diode Circuit Handbook*, Microwave Associates/HB-9000, Feb. 1971, pp. 20–24.
[4] R. L. Eisenhart and P. J. Khan, "Theoretical and experimental analysis of a waveguide mounting structure," *IEEE Trans. Microwave Theory Tech.*, vol. MTT-19, pp. 706–719, Aug. 1971.
[5] L. Lewin, "A contribution to the theory of probes in waveguides," *Proc. Inst. Elec. Eng.*, Monogr. 259R, Oct. 1957.
[6] E. C. Jordan, *Electromagnetic Waves and Radiating Systems*. London: Constable, 1962, pp. 227–228.
[7] N. Marcuvitz, *Waveguide Handbook* (M.I.T. Rad. Lab. Ser., vol. 10). New York: McGraw-Hill, 1951, pp. 258–262.

Modal Analysis of a Planar Dielectric Strip Waveguide for Millimeter-Wave Integrated Circuits

T. T. FONG, MEMBER, IEEE, AND SHUNG-WU LEE, MEMBER, IEEE

Abstract—**A novel planar waveguide which is suitable for guiding electromagnetic (EM) energy in the millimeter-wave and submillimeter-wave regions is studied. By using Wiener–Hopf techniques, we first determine the reflection coefficient at the open ends of the guide. Next, a transverse resonance condition is applied to determine the dispersion relation of the modal field. The propagation constant is found to be complex. Its imaginary part accounts for the edge diffraction loss of the strip through the open ends of the guide. Extensive numerical results are given for the disperson characteristics and modal field distributions for silicon and fuzed quartz substrates. The planar strip waveguide should have the advantages of simplicity in processing, a lower random diffraction loss, and accessibility to monolithic integration techniques.**

I. INTRODUCTION

RECENT rapid advances in millimeter-wave active and passive solid-state devices have made feasible many system applications. In order to develop a functional module for a particular system application and to reduce the size and weight of the module, an integrated circuit approach is of considerable interest. The use of a dielectric waveguide and its associated components has recently been explored in the millimeter wavelength region [1] and some encouraging results have been reported. However, the dielectric waveguide must be fabricated by chemical etching or machining, and suffers from undesirable diffraction loss and phase distortion due to random waveguide variation introduced in the fabrication process. In this paper we study the possibility of using a planar dielectric strip waveguide which does not have the preceding fabrication difficulties. As shown in Fig. 1, the geometry of the strip guide is identical to a microstrip transmission line [2]–[5] which has been widely used at microwave frequencies. Unlike the microstrip, however, the transverse dimensions of the strip guide are relatively large compared to the wavelength and therefore the guide no longer supports the TEM or quasi-TEM mode of propagation characterized by a zero cutoff frequency [2]–[5]. Consequently, despite the geometrical similarity, the modal fields of a strip guide are completely different from those of a microstrip.

It is to be stressed that the substrate thickness for a dielectric strip guide is considerably greater than for a conventional microstrip. Typically, the thickness is ten to fifteen times greater so that dominating TEM or quasi-TEM modes in the microstrip are no longer supported in the strip guide. This results from strong radiation caused by the large substrate thickness. The only modes that can still propagate in the dielectric strip guide are similar to those described by Vainshtein [6], for which the propagation constants in the transverse x direction are small and the waves undergo strong reflections at the open ends. The energy is thus trapped in the waveguide and does not radiate into the free space. Therefore, the strip guide described in this paper is entirely different from the wide microstrip configurations such as the microguide [7] or the edge mode microstrip described by Hines [8]. The greater substrate thickness is advantageous at millimeter and submillimeter wavelengths because of ease in fabrication.

Manuscript received November 5, 1973; revised March 18, 1974.
T. T. Fong is with the Hughes Research Laboratories, Torrance, Calif. 90509.
S.-W. Lee is with the Department of Electrical Engineering, University of Illinois, Urbana, Ill. 61801.

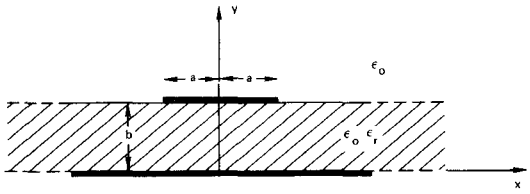

Fig. 1. Cross section of a dielectric strip guide.

Our method of analysis follows the one first introduced by Vainshtein for laser resonators [6], [9]. If the open structure in Fig. 1 is to sustain a well-defined modal field, the energy loss through the open ends at $x = \pm a$ must be small. It has been shown [9]–[11] that this is possible only when the propagation constant along the x direction is small compared with that along the y direction, and the reflection coefficient at $x = \pm a$ is only slightly less than one. Under such a condition, we can greatly simplify the expression for the reflection coefficient at $x = \pm a$ obtained by the Wiener–Hopf technique, and subsequently derive a simple dispersion relation.

II. MODAL FIELD OF TM$^{(y)}$

The cross section of the dielectric strip guide, to be analyzed in this paper, is shown in Fig. 1. It consists of a conducting strip placed on an infinite dielectric substrate backed by a perfectly conducting material. To study the modal fields guided along the z direction, it is convenient to classify the fields in two types: TM$^{(y)}$ and TE$^{(y)}$ with respect to y, a transverse direction. For TM$^{(y)}$, all the field components are derivable from a scalar potential ψ [with $\exp(-i\omega t)$ time convention suppressed]:

$$\text{TM}^{(y)}: \quad E_x = \frac{i}{\omega\epsilon}\frac{\partial^2\psi}{\partial x\,\partial y} \qquad H_x = -\frac{\partial\psi}{\partial z}$$

$$E_y = \frac{i}{\omega\epsilon}\left(\frac{\partial^2}{\partial y^2} + k_0^2\epsilon_r\right)\psi \qquad H_y = 0$$

$$E_z = \frac{i}{\omega\epsilon}\frac{\partial^2\psi}{\partial y\,\partial z} \qquad H_z = \frac{\partial\psi}{\partial x} \tag{1}$$

where $k_0 = \omega(\mu\epsilon_0)^{1/2} = 2\pi/\lambda_0$ is the wavenumber in free space. In this and the next section, we shall concentrate on the study of TM$^{(y)}$ modes.

First let us consider a special case with $a \to \infty$ (Fig. 1), which results in a conventional parallel plate waveguide filled with a dielectric medium ϵ_r. Then the potential for TM$_{mn}^{(y)}$ mode assumes the familiar form:

$$\psi_{mn} = \exp(i\alpha_m x)\cos\left(\frac{n\pi}{b}y\right)\exp(i\beta_{mn}z) \tag{2}$$

where α_m, and β_{mn} are, respectively, the propagation constants along the x and z directions; they satisfy the dispersion relation

$$\alpha_m^2 + \left(\frac{n\pi}{b}\right)^2 + \beta_{mn}^2 = k_0^2\epsilon_r. \tag{3}$$

For a finite a, instead of a traveling wave, there should be a standing wave along the x direction, namely

$$\psi_{mn} = [\exp(i\alpha_m x) + R_{mn}\exp(i2\alpha_m a)\exp(-i\alpha_m x)] \cdot\cos\frac{n\pi}{b}y\exp(i\beta_{mn}z) \tag{4}$$

where R_{mn} may be identified as the reflection coefficient at the open ends $x = \pm a$, and will be studied in the next section. To sustain a modal solution in the present open structure, the well-known transverse resonance condition requires [6]

$$R_{mn}\exp(i2\alpha_m a) = \exp[i(m+1)\pi], \qquad m = 1,2,3,\cdots. \tag{5}$$

Alternatively, it may be written as

$$\alpha_m = \left[\frac{m\pi}{2a} + i\frac{1}{2a}\ln(-R_{mn})\right]. \tag{6}$$

Using (5) in (4), we obtain the formal solution for TM$_{mn}$ mode in the structure shown in Fig. 1:

$$\psi_{mn} = \begin{cases}\cos\alpha_m x & m = 1,3,5\cdots \\ \sin\alpha_m x & m = 2,4,6\cdots.\end{cases}\cos\frac{n\pi}{b}y\exp(i\beta_{mn}z), \tag{7}$$

where the multiplication constants have been omitted. Thus, for a given guide dimension (a,b) and dielectric constant ϵ_r, the propagation constant β_{mn} can be determined from (3) and (6) once R_{mn} is known.

III. DISPERSION RELATION OF TM$^{(y)}$

For the geometry depicted in Fig. 1, it does not appear that the reflection coefficient R_{mn} at junction $x = \pm a$ lends itself to a closed form solution. In the following we shall introduce two approximations.

1) We shall neglect the coupling between the two open ends at $x = \pm a$. This is valid when $2a$ is large in terms of the transverse wavenumber, i.e.,

$$2k_0 a\,|\,[\epsilon_r - (\beta/k_0)^2]^{1/2}\,| \gg 1.$$

Under this approximation, for the purpose of determining R_{mn} at $x = a$, the problem in Fig. 1 can be replaced by that in Fig. 2, namely, a semi-infinite strip extended from $x = 0$ to $x = -\infty$. It can be shown that TM$^{(y)}$ and TE$^{(y)}$ are coupled and therefore it is a three-dimensional vector field problem. To facilitate the application of the Wiener–Hopf technique to obtain an analytic solution, we shall introduce another approximation.

2) In matching the tangential fields at the interface $y = b$ (Fig. 2), only the conditions on (E_z,H_x) will be enforced while those on (E_x,H_z) will be neglected. This approximation is reasonable because for TM$^{(y)}$ mode, the dominant components are $(E_y, E_z,$ and $H_x)$, while (E_x,H_z) being proportional to α_m are small.

With the approximations stated in 1) and 2), we have equivalently a two-dimensional scalar problem at hand.

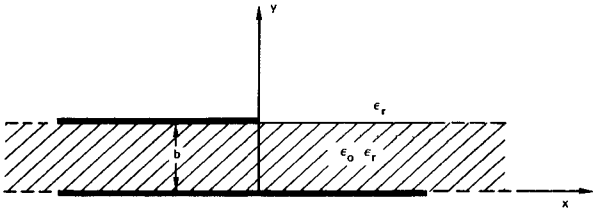

Fig. 2. Parallel plate waveguide for determining R_{mn}.

The solution of the reflection coefficient R_{mn} can be found by the Wiener–Hopf technique. Since the detailed analysis of a similar problem has been presented elsewhere [9], [10] we shall only give the final result as follows:

$$R_{mn} = [\alpha_m + (k_0^2\epsilon_r - \beta_{mn}^2)^{1/2}]^2 \frac{G_+^2(\alpha_m)}{2\alpha_m^2}. \tag{8}$$

In standard Wiener–Hopf notation, $G_+(\alpha)$ is the "plus part" of a Wiener–Hopf kernel $G(\alpha)$, which is given by

$$G(\alpha) = \frac{\Gamma}{\gamma b(\Gamma + \epsilon_r\gamma \coth \Gamma b)} \tag{9}$$

where

$$\Gamma = +[\alpha^2 - (k_0^2\epsilon_r - \beta_{mn}^2)]^{1/2} = -i[(k_0^2\epsilon_r - \beta_{mn}^2) - \alpha^2]^{1/2} \tag{10}$$

$$\gamma = +[\alpha^2 - (k_0^2 - \beta_{mn}^2)]^{1/2} = -i[(k_0^2 - \beta_{mn}^2) - \alpha^2]^{1/2}. \tag{11}$$

A direct use of (9) will lead to a result which is too complicated to be useful. Thus, in the following, we shall seek a simplified form of (9) with the appropriate approximations.

In order to support a propagating mode in the structure in Fig. 1 with small loss (Im $\beta_{mn} \ll 1$) it is necessary that the reflection coefficient R_{mn} has a magnitude close to unity. It has been shown by Vainshtein [6] and Bates [11] that this is possible only when $|\alpha_m|^2 \ll (n\pi/b)^2$. In view of this and (3), it is convenient to introduce a parameter P_m such that

$$[k_0^2\epsilon_r - \beta_{mn}^2]^{1/2}b = \pi(n + P_m). \tag{12}$$

Thus, instead of dealing with α_m, we shall work with P_m, a complex number with magnitude $|P_m| \ll 1$, and

$$\frac{\alpha_m}{(k_0^2\epsilon_r - \beta_{mn}^2)^{1/2}} \approx \left(\frac{2P_m}{n}\right)^{1/2} \ll 1. \tag{13}$$

Realizing the fact that $\alpha = \alpha_m$ is used for the calculation of R_{mn} in (8), we invoke the following approximations for Γ and γ defined in (10) and (11):

$$\Gamma \approx -i(k_0^2\epsilon_r - \beta_{mn}^2)^{1/2}\left[1 - \frac{\alpha^2}{2(k_0^2\epsilon_r - \beta_{mn}^2)}\right] \tag{14}$$

$$\gamma \approx -i(k_0^2 - \beta_{mn}^2)^{1/2}. \tag{15}$$

Then the Wiener–Hopf kernel $G(\alpha)$ in (9) becomes

$$G(\alpha) \approx \left\{i \Big/ \left[(k_0^2 - \beta_{mn}^2)^{1/2} \cdot b\left(1 + \epsilon_r \frac{(k_0^2 - \beta_{mn}^2)^{1/2}}{(k_0^2\epsilon_r - \beta_{mn}^2)^{1/2}}\right)\right]\right\} \frac{M(\alpha,1)}{M(\alpha,c)}. \tag{16}$$

In the preceding, we have used the notation

$$M(\alpha,c) = 1 - c \exp\left\{i2(k_0^2\epsilon_r - \beta_{mn}^2)^{1/2} \cdot b\left[1 - \frac{\alpha^2}{2(k_0^2\epsilon_r - \beta_{mn}^2)}\right]\right\} \tag{17}$$

where

$$c = \frac{1 - \epsilon_r[(k_0b/n\pi)^2(1 - \epsilon_r) + 1]^{1/2}}{1 + \epsilon_r[(k_0b/n\pi)^2(1 - \epsilon_r) + 1]^{1/2}}. \tag{18}$$

The factorization of $M(\alpha,1)$ was discussed by Vainshtein [6] and $M(\alpha,c)$ by the authors [9]. The results are

$$M_+(\alpha_m,1) \approx (8\pi P_m)^{1/2} \exp[-0.824(1 - i)(\pi P_m)^{1/2}] \tag{19}$$

$$M_+(\alpha_m,c) \approx (1 - c)^{1/2} \exp\left[(1 - i)(P_m)^{1/2} \sum_{q=1}^{\infty} \frac{c^q}{q^{1/2}}\right]. \tag{20}$$

Formulas in (19) and (20) are excellent approximations for real $c < 1$ and $P_m < 0.25$. A detailed discussion on the accuracy of these formulas was given in [9]. However, in the present analysis, we are also interested in situations where c is complex and $|c| \approx 1$. In such cases, the series in (20) converges slowly. For numerical calculation, a better representation of $M_+(\alpha_m,c)$ is given by an integral over a steepest descent path [9], namely,

$$\ln M_+(\alpha_m,c) = \frac{1}{2\pi i}\int_{-\infty}^{\infty} \frac{\ln\{1 - c \exp[i2\pi P_m - (t^2/2)]\}}{t - \alpha_m(b/k_0)^{1/2} \exp(i\pi/4)}\, dt. \tag{21}$$

Substituting (13)–(20) and (21) into (8), after simplification, we obtain the desired expression for the reflection coefficient for the $TM_{mn}^{(y)}$ mode:

$$R_{mn} = (-1) \exp[i(4\pi P_m)^{1/2}(1 + i)0.824g_0]. \tag{22}$$

Here we have two expressions for g_0. For real $c < 1$, we use

$$g_0 = 1 + \frac{1}{0.824(\pi)^{1/2}} \sum_{q=1}^{\infty} \frac{c^q}{q^{1/2}}. \tag{23}$$

For complex c, we use

$$g_0 = 1 + \frac{(1 + i)}{0.824(4\pi P_m)^{1/2}}[U(c,P_m) - \tfrac{1}{2}\ln(1 - c)] \tag{24}$$

where

$$U(c,P_m) = \frac{1}{2\pi i}\int_{-\infty}^{\infty} \frac{\ln\{1 - \exp[i2\pi P_m + \ln[c/(1-c)^{1/2}] - t^2/2]\}}{t - (4\pi P_m)^{1/2}\exp(i\pi/4)}\,dt.$$

The formula in (22) is valid under the assumptions 1) and 2). For the special case where the dielectric is absent ($\epsilon_r = 1$), g_0 reduces to unity. Thus g_0 may be considered the filling factor accounting for the dielectric loading.

With the reflection coefficient R_{mn} found in the preceding, and with the aid of the dispersion relation given in (3) and (6), P_m may be written as

$$P_m = \frac{\pi m^2}{4[(2\pi n)^{1/2}(a/b) + (1+i)0.824g_0]^2}. \tag{25}$$

For given waveguide parameters (k_0a, k_0b, ϵ_r) and given mode index (m,n), we may calculate the complex number P_m from (25). It should be noted that for real $c < 1$, g_0 given in (23) is independent of P_m, and (25) determines P_m explicitly. For complex c, g_0 is a function of P_m, and P_m must be solved by iteration. The propagation constants (α_m,β_{mn}) along (x,z) directions follow from (12) and (13) or equivalently

$$\frac{\alpha_m}{k_0} = \frac{\pi}{k_0 b}[P_m(2n + P_m)]^{1/2} \tag{26}$$

$$\frac{\beta_{mn}}{k_0} = \left[\epsilon_r - \left(\frac{\pi(n+P_m)}{k_0 b}\right)^2\right]^{1/2} \tag{27}$$

where β_{mn} is a complex number, and its small positive imaginary part accounts for the radiation loss at the open ends $x = \pm a$.

IV. RESULTS FOR TE$^{(y)}$

The analysis of TE$^{(y)}$ modes follows exactly the same procedures as those for TM$^{(y)}$ modes presented in Sections II and III. In the following, we shall only summarize the final results. The field components of TE$^{(y)}$ are derivable from scalar potential $\bar{\psi}$ as follows:

$$\text{TE}^{(y)}: \quad E_x = \frac{\partial\bar{\psi}}{\partial z} \qquad H_x = \frac{i}{\omega\mu}\frac{\partial^2\bar{\psi}}{\partial x\,\partial y}$$

$$E_y = 0 \qquad H_y = \frac{i}{\omega\mu}\left(\frac{\partial^2}{\partial y^2} + k_0^2\epsilon_r\right)\bar{\psi}$$

$$E_z = -\frac{\partial\bar{\psi}}{\partial x} \qquad H_z = \frac{i}{\omega\mu}\frac{\partial^2\bar{\psi}}{\partial y\,\partial z}. \tag{28}$$

For the TE$_{mn}^{(y)}$ mode, $\bar{\psi}$ takes the form of

$$\bar{\psi}_{mn} = \begin{Bmatrix}\cos\bar{\alpha}_m x \\ \sin\bar{\alpha}_m x\end{Bmatrix} \sin\frac{n\pi}{b}y\exp(i\bar{\beta}_{mn}z) \qquad \begin{matrix} m = 1,3,5\cdots \\ m = 2,4,6\cdots. \end{matrix} \tag{29}$$

The propagation constants $(\bar{\alpha}_m,\bar{\beta}_{mn})$ again can be computed from (23)–(26), except that c should be replaced by $\bar{c}$, and

$$\bar{c} = \frac{[(k_0b/n\pi)^2(1-\epsilon_r) + 1]^{1/2} - 1}{[(k_0b/n\pi)^2(1-\epsilon_r) + 1]^{1/2} + 1}. \tag{30}$$

Since $\bar{\alpha}_m$ is small, the dominant components of the TE$^{(y)}$ mode are (E_x,H_y,H_z).

V. NUMERICAL RESULTS AND DISCUSSION

In numerical calculations, the complex constants P_m are solved from (25) by means of iteration as described in the following. Using an initial value of g_0 generated by (23), a first order P_m is calculated from (25), and an improved g_0 from (24). Substitute the improved g_0 in (25), we have a second order P_m. The procedure repeats until the variation of P_m becomes less than a preset error criterion. Typically, this procedure yields a variation in P_m within 0.1 percent by only two to six iterations.

In Figs. 3(a)–6(a), the calculated propagation constant Re β_{mn} from (27) is plotted as functions of b/λ_0 for four lowest order TM$_{mn}^{(y)}$ and TE$_{mn}^{(y)}$ modes with aspect ratio $(a/b) = 1$ and 2, for $\epsilon_r = 11.8$ (high resistivity silicon) and $\epsilon_r = 3.78$ (fuzed quartz). It is observed that the strip guide analyzed in the present paper has dispersion characteristics very similar to those of the dielectric guide [12], [13].

1) The separation between modes decreases as the aspect ratio (a/b) or dielectric constant ϵ_r increases.

2) TM$_{mn}^{(y)}$ and TE$_{mn}^{(y)}$ have practically the same propagation constants Re β_{mn}. The reason that the presence of the dielectric loading in our study does not remove this degeneracy is because, for the transverse resonance condition to satisfy, P_m has to be small, meaning that the incident plane wave, the first term of (4) at $y = b$ in Fig. 1, is nearly perpendicular to the dielectric interface (i.e., normal incidence). In which case, it is known that the refraction at the dielectric interface is independent of polarization.

A striking difference between the present analysis and those for optical and microwave open guides is that we are able to calculate the attenuation constant Im β_{mn}. For an open structure shown in Fig. 1, even under ideal conditions (lossless dielectric and conductor), the EM energy cannot be confined perfectly due to the radiation loss caused by diffraction at $(x = \pm a, y = b)$. This loss is reflected in the positive imaginary part of β_{mn}. We have calculated Im β_{mn} from (27) and the results are given in Figs. 3(b)–6(b). The following observations can be made.

1) The radiation loss decreases as the aspect ratio (a/b) ϵ_r increases.

2) The radiation loss increases as Re β_{mn} decreases. At Re $\beta_{mn} = k_0$, the major portion of the modal energy is no longer confined in the waveguide and the radiation loss increases sharply.

3) The lowest radiation loss is associated with the mode which has the smallest transverse propagation constant

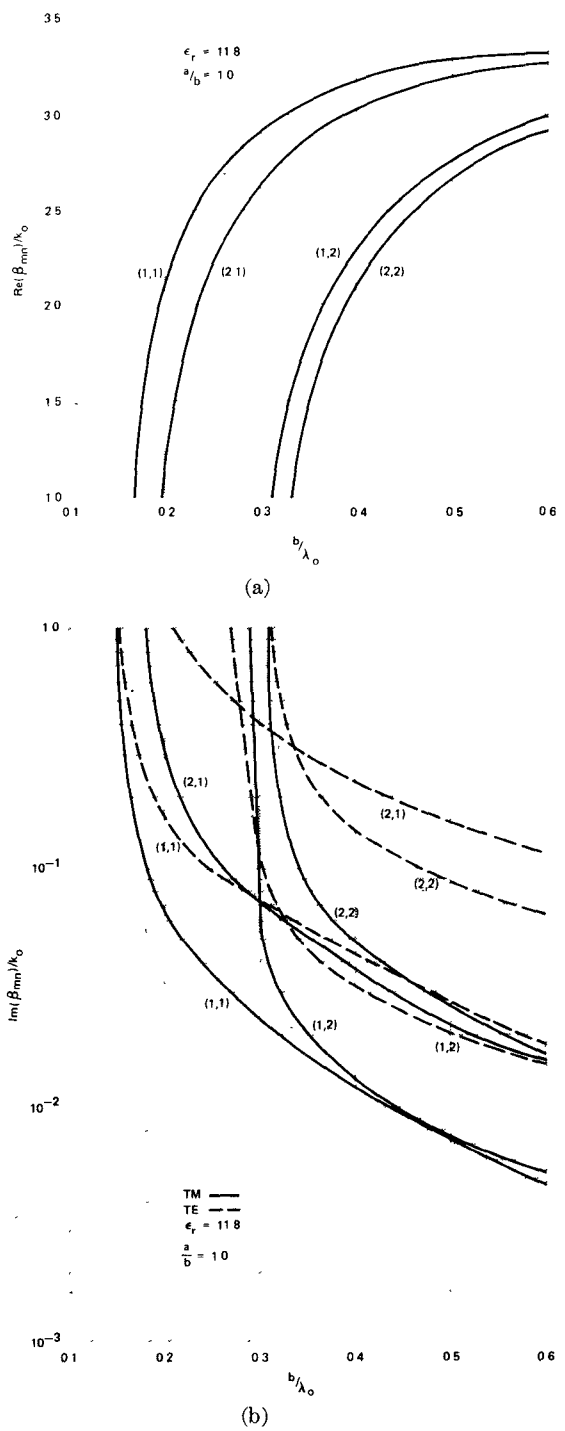

Fig. 3. Normalized propagation and attenuation constants of four lowest order modes for high resistivity silicon substrate; $\epsilon_r = 11.8$, $a/b = 1.0$.

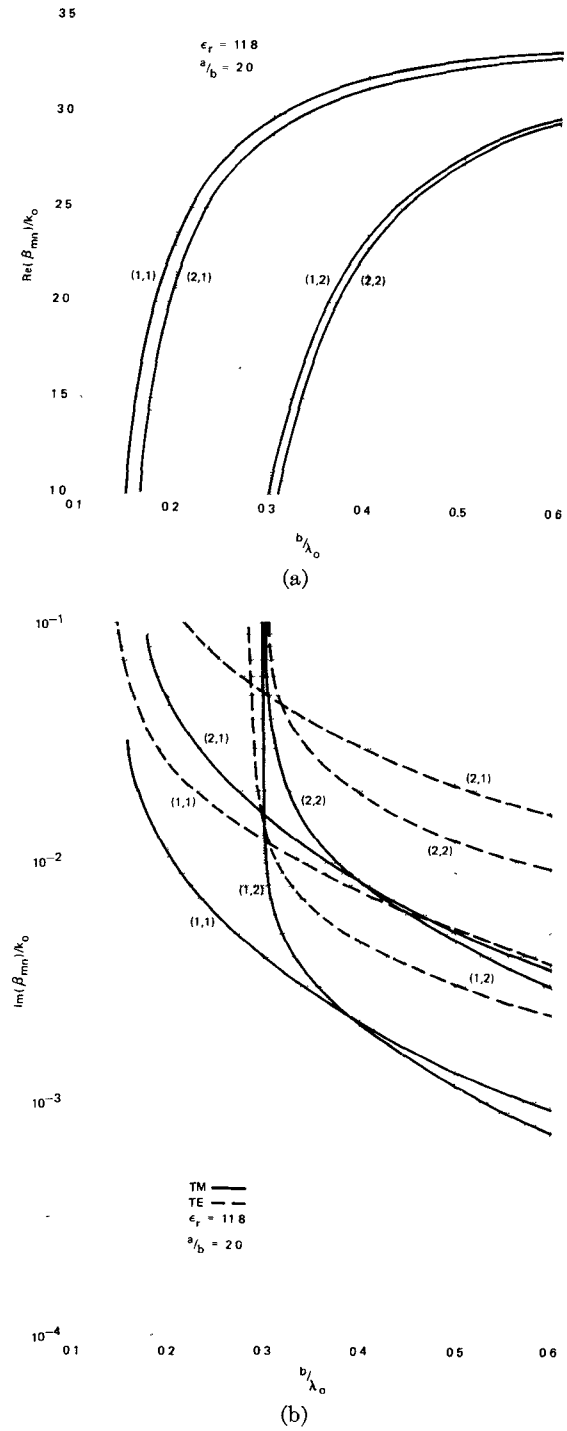

Fig. 4. Normalized propagation and attenuation constants of four lowest order modes for high resistivity silicon substrate; $\epsilon_r = 11.8$, $a/b = 2.0$.

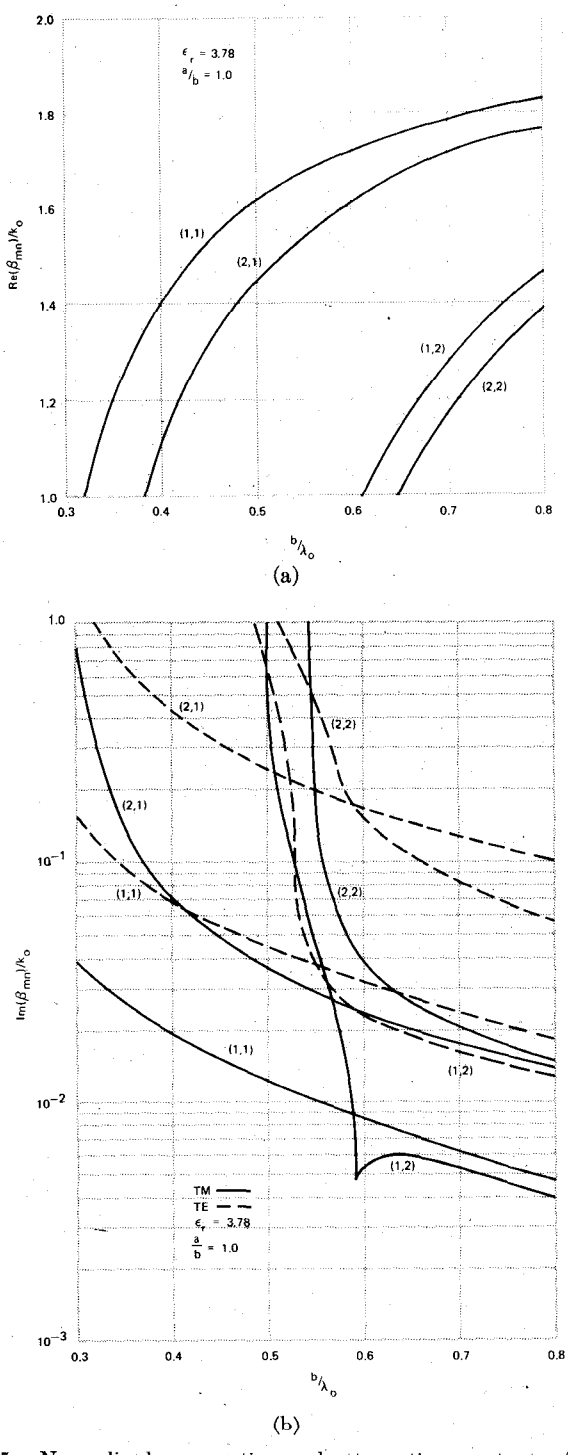

Fig. 5. Normalized propagation and attenuation constants of four lowest order modes for fused quartz substrate; $\epsilon_r = 3.78$, $a/b = 1.0$.

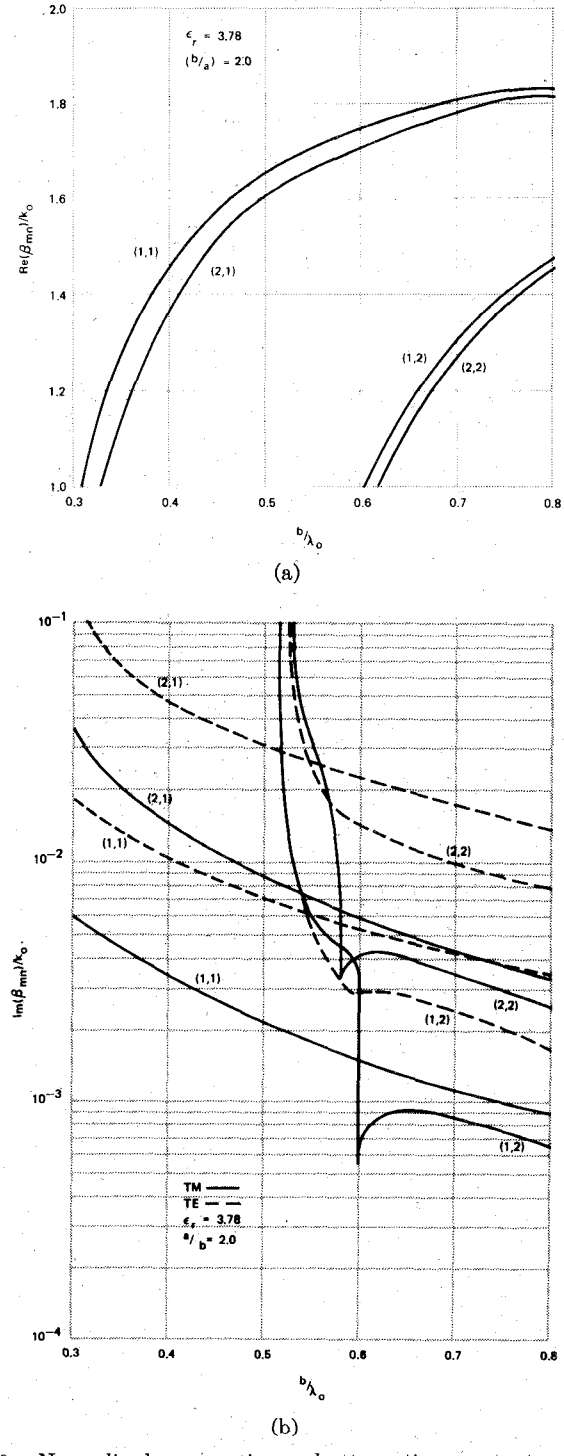

Fig. 6. Normalized propagation and attenuation constants of four lowest order modes for fused quartz substrate; $\epsilon_r = 3.78$, $a/b = 2.0$.

α_m [6], [11]. As b/λ_0 increases, the smaller α_m come from modes with higher indices. Consequently, the attenuation constant of a lower indexed mode may cross over that of a higher index.

4) Figs. 5(b) and 6(b) also manifest the competing effects of dielectric loading and edge diffraction. For waveguides with relatively high dielectric constants, the modal fields are quite confined due to the dielectric loading and the edge diffraction is less predominant. However, as the dielectric constant decreases, the edge diffraction becomes the predominating mechanism responsible for radiation loss. Thus, for certain modes, such as the $TM_{1,2}^{(y)}$ mode, the diffraction loss is at a minimum for $n = 2$ at $b/\lambda_0 \approx 0.6$ [Figs. 5(b) and 6(b)] because of $\alpha_m \approx 0$, and the lowest diffraction loss is associated with the mode just slightly above cutoff. Either below or above this b/λ_0, the loss increases owing to the critical diffraction at the open ends.

It should also be mentioned that in computing the propagation constants and attenuation constants for $k_0 \approx \beta_{mn}$, the approximation as defined by (15) is no longer valid. Instead, one should use

$$\gamma \approx -i[k_0^2 - \beta_{mn}^2 - (\pi/b)^2 2nP_m]^{1/2}. \tag{31}$$

Consequently,

$$c(P_m) = \frac{1 - \epsilon_r Q}{1 + \epsilon_r Q}, \qquad \text{for } TM_{mn}^{(y)} \text{ modes} \tag{32}$$

$$\bar{c}(P_m) = \frac{Q - 1}{Q + 1}, \qquad \text{for } TE_{mn}^{(y)} \text{ modes} \tag{33}$$

where

$$Q = [(k_0 b/n\pi)^2(1 - \epsilon_r) + 1 - 2P_m]^{1/2}.$$

Therefore, for $k_0 \approx \beta_{mn}$, both c and $\bar{c}$ become functions of P_m, and g_0 can only be obtained by iteration as previously described.

Transverse field distribution for different modes may be calculated from (1) and (2) for $TM^{(y)}$ and (29) for $TE^{(y)}$. Such distributions along the x direction are presented in Figs. 7–10 for $TM^{(y)}$ modes. Field distributions for $TE^{(y)}$ modes are not shown because they are similar to the $TM^{(y)}$ modes owing to the degeneracy in Re β_{mn}. It is seen that the field distributions in the strip guide are similar to those of laser resonators [6], [9]. The nonzero value of the field at $x = \pm a$ is related to the radiation loss, the higher the field value generally results a higher radiation loss. This observation may be verified, for example, by comparing Fig. 8 ($|f(a)| \approx 0.29$, Im $\beta_{11} \approx 7 \times 10^{-3} k_0$ for $a/b = 1$) and Fig. 10 ($|f(a)| \approx 0.43$, Im $\beta_{11} \approx 10^{-2} k_0$ for $a/b = 1$).

In addition to the diffraction loss discussed above, another dominant loss mechanism comes from the finite conductivity of the guide walls. To obtain a first order approximation of the latter loss, let us assume that the conductivity of the guide walls is sufficiently high at the frequency range of interest. Thus the field distributions are not significantly altered by the presence of the ohmic loss. In which case, the complex propagation constant due to ohmic loss can be written as

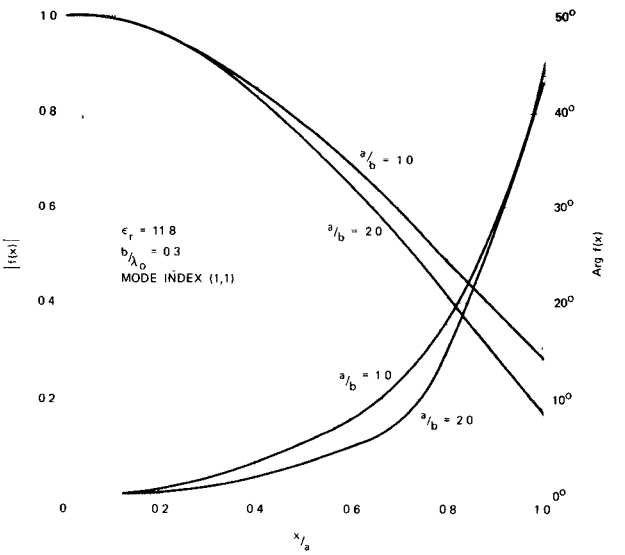

Fig. 7. Field distribution along x direction: $f(x) = \cos \alpha_1 x$ for $TM_{11}^{(y)}$; $\epsilon_r = 11.8$, $b/\lambda_0 = 0.3$.

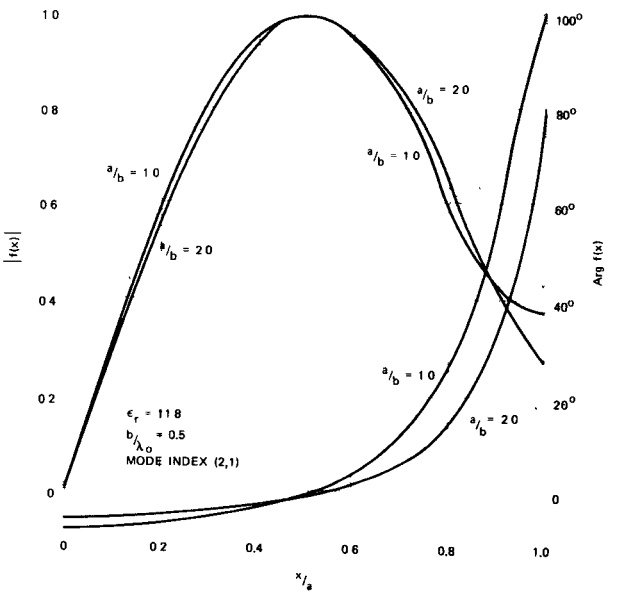

Fig. 8. Field distribution along x direction: $f(x) = \sin \alpha_2 x$ for $TM_{21}^{(y)}$; $\epsilon_r = 11.8$, $b/\lambda_0 = 0.5$.

$$\beta_{\text{ohmic}} = i \frac{1}{\Phi} \frac{d\Phi}{dz} \tag{34}$$

where

$$\Phi = \oiint E \times H^* \cdot d\boldsymbol{S}$$

$$\frac{d\Phi}{dz} = \frac{R_s}{2} \oint |H_{\tan}|^2 \, dl.$$

$R_s = (\omega\mu_0/2\sigma)^{1/2}$ is the surface resistance due to finite conductivity of the metallic strip and ground plane. $H_{\tan}$, in a first order approximation, are set equal to the nondissipative magnetic field components tangential to the guide periphery. The line integral with respect to dl extends over the metallic guide periphery and the surface integral extends over the transverse waveguide cross section. Following from (1), (7), (28), and (29), after simplification one obtains the following for $TM_{mn}^{(y)}$ modes:

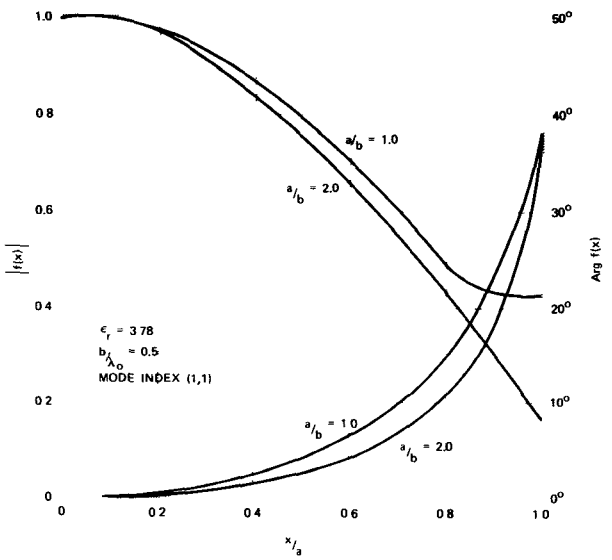

Fig. 9. Field distribution along x direction: $f(x) = \cos \alpha_1 x$ for $TM_{11}^{(y)}$; $\epsilon_r = 3.78$, $b/\lambda_0 = 0.5$.

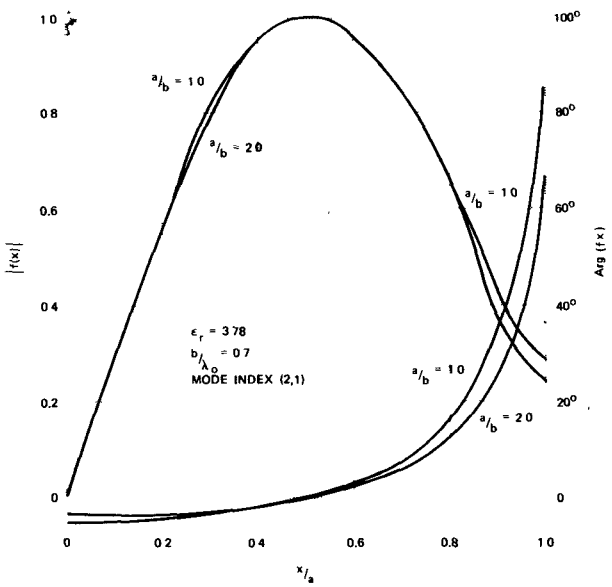

Fig. 10. Field distribution along x-direction: $f(x) = \sin \alpha_2 x$ for $TM_{21}^{(y)}$; $\epsilon_r = 3.78$, $b/\lambda_0 = 0.7$.

$$\beta_{\text{ohmic}} = \frac{iR_s\omega\epsilon_r\epsilon_0}{\pi(\beta_{mn}/k_0)\,(b/\lambda_0)} f(\alpha_m,\beta_{mn}) \tag{35}$$

for $TE_{mn}^{(y)}$ modes,

$$\bar{\beta}_{\text{ohmic}} = \frac{iR_s\omega\mu(n\pi/b)^2}{\pi(\bar{\beta}_{mn}/k_0)\,(b/\lambda_0)} f(\bar{\alpha}_m,\bar{\beta}_{mn}) \tag{36}$$

where

$$f(\alpha_m,\beta_{mn}) = \frac{1 + (-1)^m \dfrac{\alpha_m^2 - \beta_{mn}^2}{\alpha_m^2 + \beta_{mn}^2} \dfrac{\sin 2\alpha_m a}{2\alpha_m a}}{1 - (-1)^m \dfrac{\sin 2\alpha_m a}{2\alpha_m a}}. \tag{37}$$

For propagating modes not close to cutoff, or $\beta_{mn} > k_0$, we have $\alpha_m^2 \ll \beta_{mn}^2$ and $f(\alpha_m,\beta_{mn}) \approx 1$. Thus the ohmic loss can be readily calculated once β_{mn}/k_0 is known. As a numerical example, let us consider the case with $\epsilon_r = 11.8$, $b/\lambda_0 = 0.3$, and $a/b = 2.0$. From Fig. 3, we have $\beta_{mn}/k_0 = 2.98 + i3.94 \times 10^{-3}$. If we choose a frequency of 60 GHz and the metal to be copper with $\sigma = 4.0 \times 10^9$ mho/cm, the surface resistance is $R_s = 7.7 \times 10^{-2}\ \Omega$ and $\beta_{\text{ohmic}} = 1.09 \times 10^{-2}$ Np/cm. If this is compared with the radiation loss $\text{Im}\,\beta_{mn} = 3.94 \times 10^{-3} k_0 = 4.95 \times 10^{-2}$ Np/cm, we conclude, for this case, the dominant loss factor is from radiation with the conduction loss amounts to about 20 percent of the radiation loss. The high radiation loss may provide a plausible explanation of the fact that the measured guided wavelength for dielectric waveguide at low aspect ratio does not agree with existing theoretical predictions [14].

VI. CONCLUSION

A planar dielectric strip waveguide operating at millimeter-wave has dispersion characteristics similar to those of a dielectric waveguide, but the strip waveguide is more easily fabricated and integrated with other components. The radiation loss at the open ends of the guide dominates over the conduction loss for copper walls, and therefore is an important factor in the design of a strip guide. Though the discussion in this paper has been focused on the millimeter-wave, we believe the strip waveguide can also be used at optical frequencies. Proper metallization similar to that used in an optical mirror, however, may be necessary to minimize the conduction loss.

REFERENCES

[1] H. Jacobs and M. M. Chrepta, "Semiconductor dielectric waveguide for millimeter-wave functional circuits," in *Dig. Tech. Papers, 1972 IEEE G-MTT Int. Microwave Symp.* (Denver, Colo.), June 1973, pp. 28–29.
[2] P. Daly, "Hybrid-mode analysis of microstrip by finite-element methods," *IEEE Trans. Microwave Theory Tech.*, vol. MTT-19, pp. 19–25, Jan. 1971.
[3] E. J. Denlinger, "A frequency dependent solution of microstrip transmission lines," *IEEE Trans. Microwave Theory Tech.*, vol. MTT-19, pp. 30–39, Jan. 1971.
[4] R. Mittra and T. Itoh, "A new technique for the analysis of the dispersion characteristics of microstrip lines," *IEEE Trans. Microwave Theory Tech.*, vol. MTT-19, pp. 47–56, Jan. 1971.
[5] T. Itoh and R. Mittra, "Spectral-domain approach for calculating the dispersion characteristics of microstrip lines," *IEEE Trans. Microwave Theory Tech.*, vol. MTT-21, pp. 496–499, July 1973.
[6] L. A. Vainshtein, "Open resonators for lasers," *Sov. Phys.—JETP*, vol. 17, pp. 709–719, Sept. 1963.
[7] E. G. Cristal, A. F. Podell, and D. Parker, "Microguide, a new microwave integrated circuit transmission line," in *Dig. Tech. Papers, 1972 IEEE G-MTT Int. Microwave Symp.* (Arlington Heights, Ill.), May 1972, pp. 149–151.
[8] M. E. Hines, "Reciprocal and nonreciprocal modes of propagation in ferrite stripline and microstrip devices," *IEEE Trans. Microwave Theory Tech.*, vol. MTT-19, pp. 442–451, May 1971.
[9] T. T. Fong and S. W. Lee, "Theory of Fabry-Perot resonators with dielectric medium," *IEEE J. Quantum Electron.*, vol. QE-7, pp. 1–11, Jan. 1971.
[10] R. Mittra and S. W. Lee, *Analytical Techniques in the Theory of Guided Waves*. New York: Macmillan, 1971, ch. 3.
[11] C. P. Bates, "Internal reflection at the open end of a semi-infinite waveguide," *IEEE Trans. Antennas Propagat.*, vol. AP-18, pp. 230–235, Mar. 1970.
[12] E. A. J. Marcatili, "Dielectric rectangular waveguide and directional coupler for integrated optics," *Bell Syst. Tech. J.*, vol. 48, pp. 2071–2102, Sept. 1969.
[13] J. E. Goell, "A circular-harmonic computer analysis of rectangular dielectric waveguide," *Bell Syst. Tech. J.*, vol. 48, pp. 2133–2160, Sept. 1969.
[14] R. M. Knox and P. P. Toulios, "Integrated circuits for the millimeter through optical frequency range," in *Dig. Symp. on Submillimeter-Waves* (Polytechn. Inst. Brooklyn, N. Y.), Mar. 1970, pp. 497–516.